Mechanical Systems and Signal Processing 139 (2020) 106654

Contents lists available at ScienceDirect

Mechanical Systems and Signal Processing

journal homepage: www.elsevier.com/locate/ymssp

Real-time defect detection of high-speed train wheels by using Bayesian forecasting and dynamic model

Y.W. Wang [a,b], Y.Q. Ni [a,b,*], X. Wang [a,b]

[a] Department of Civil and Environmental Engineering, The Hong Kong Polytechnic University, Hung Hom, Kowloon, Hong Kong
[b] National Rail Transit Electrification and Automation Engineering Technology Research Center (Hong Kong Branch), Hung Hom, Kowloon, Hong Kong

ARTICLE INFO

Article history:
Received 2 September 2019
Received in revised form 4 January 2020
Accepted 13 January 2020
Available online 25 January 2020

Keywords:
High-speed train
Wheel
Defect detection
Bayesian dynamic linear model (DLM)
Bayesian forecasting

ABSTRACT

High-speed rail (HSR) is being developed in Asian and European countries to satisfy the rapidly growing demand for intercity services and to shore up economic growth. The rapid growth of HSR, however, has posed great challenges regarding operation safety, reliability and ride comfort. Irregular wheel defects can induce high-magnitude impact forces hindering safety and ride comfort of HSR and may also cause damage to rail tracks and vehicles. The focus of this study is to develop a real-time defect detection methodology based on Bayesian dynamic linear model (DLM) enabling to detect potentially defective wheels in real time. The proposed methodology embraces logics for (i) prognosis, (ii) potential outlier detection, (iii) identification of change occurrence (change-point detection), and (iv) quantification of damage extent and uncertainty. Relying on the strain monitoring data acquired from high-speed train bogies, the Bayesian DLM for characterizing the actual stress ranges is established, by which one-step forecast distribution is elicited before proceeding to the next observation. The detection of change-point is executed by comparing the routine model (forecast distribution generated by the Bayesian DLM) and an alternative model (the mean value is shifted by a prescribed offset) to determine which better fits the actual observation. If the comparison results are in favor of the alternative model, it is claimed that a potential change has occurred. Whether such an observation is an outlier or the beginning of a genuine change (change-point), three metrics (i.e., Bayes factor, maximum cumulative Bayes factor and run length) are performed for further identification. Once a change-point is confirmed, Bayesian hypothesis testing is conducted for the purpose of damage extent assessment and uncertainty quantification. A severe change, if identified, implies that the quality of train wheels has suffered from a significant alteration due to defects. In the case study, two cases making use of strain monitoring data acquired by fiber Bragg grating (FBG) sensors affixed on bogies are illustrated to verify the performance of the proposed methodology for real-time wheel defect detection of in-service high-speed trains.

1. Introduction

The rapid development of high-speed rail (HSR) has enhanced convenience and mobility, but paralleling this comparatively new transport mode is a growing concern about operation safety as well as an annually increasing budget for inspec-

* Corresponding author at: Department of Civil and Environmental Engineering, The Hong Kong Polytechnic University, Hung Hom, Kowloon, Hong Kong.
E-mail address: ceyqni@polyu.edu.hk (Y.Q. Ni).

https://doi.org/10.1016/j.ymssp.2020.106654
0888-3270/

tion and maintenance work to prevent potential accidents. Rail accidents were occasionally caused by failures such as severe defects or fatigue of railway components. To maintain a good service quality and operation safety, it is paramount to develop online monitoring techniques that not only quickly recognize faults of mission-critical HSR components but also can anticipate of long-term mechanisms and gradual deterioration in performance.

Wheelsets in a high-speed train are physically connected with and controlled by the bogie system which corrects alignment for stable running and reduces the vibration caused by wheel-rail interaction [1,2]. However, the wheel performance progressively deteriorates in different mechanisms (e.g., wheel flat and wheel polygonization) during the routine operation of a high-speed train [3,4]. Wheel performance deterioration increases stresses experienced by the bogie system. In addition, the increased stress within bogie frames caused by wheel quality deterioration can be unexpectedly large, thus posing a serious threat to the operation safety of concerned trains. According to the statistics of train accidents caused by failure in mechanical components during 2004 to 2007 in the United States, the wheelsets faults are the most cause with a rate of 44.7% [5]. Therefore, the railway managers are keen to keep wheels in an adequate condition and detect potential failure as soon as possible. For railway wheels, there are three different ways of estimating the conditions: physical modeling [6,7], statistical modeling [8] and condition monitoring [9]. However, the first two ways are not applicable to in-service wheel condition assessment, and in contrast, the third way is most feasible for wheel condition estimation. The monitoring approaches available to wheel defect detection can be divided into in-workshop inspection and in-service detection [9]. The latter provides the real-time data required for maintenance planning, while the former is normally carried out at workshops at fixed intervals. The commonly used in-workshop methods for wheel defect inspection include the ultrasonic techniques [10], infrared camera [11] and magnetic methods [12]. In-service monitoring approaches can be categorized as on-board and wayside methods. The on-board methods implement sensors on the train and continuously obtain comprehensive data from the system. The methods of this category include magnetic technique [13], ultrasonic technique [14], acoustic technique [15], and vibration technique [16]. On the other hand, wayside methods attempt to detect the wheel or vehicle performance by installing sensors on the rail or its surrounding areas. Such indirect measurements give rise to limited information of the wheel condition while they can monitor all train wheels going by with using only one or a few sensors. According to the type of sensors used, wayside detection approaches include strain sensing technology [17], fiber optic sensing technology [18], ultrasonic technique [19], vibration technique [20], acoustic emission [21], lasers and high-speed cameras [22]. However, the study on data interpretation techniques enabling the extraction of defect-sensitive features is far from sufficient.

Bayesian dynamic linear model (DLM) is an elegant system approach to handling time series data from a Bayesian perspective, which originates from the field of applied statistics [23,24] and is extensively used in other fields such as economics and engineering [25–30]. The Bayesian DLM treats the time series as the output of a dynamic system perturbed by random disturbances. It is suitable for modeling both univariate and multivariate time series, and also for representing the structural changes, non-stationarity and irregular patterns [31]. Unlike the classical time series method which assumes a fixed relationship between the dependent variables (response variables) and the independent variables (regressors), the DLM considers the relationship changes over time and is able to directly capture time series data features, such as trend, seasonality, and regression effects. Moreover, the DLM allows for descriptions of temporary or permanent shifts in time series parameters that occur abruptly, which are necessary for outlier and damage detection in structural health monitoring (SHM) paradigms. Recently, Goulet and his collaborator [32,33] adopted the Bayesian DLM theory in SHM to model the time-dependent responses of structures by breaking them into subcomponents. In the perspective of real-time damage detection, only few studies are available. The first attempt was conducted by Lipowsky et al. [25] with the development of a Bayesian DLM-based real-time detection algorithm to evaluate the performance of a gas turbine using simulated data. Later on, Wang et al. [34] and Zhang et al. [35] adopted the above algorithm for detecting high-speed train defects by using real-world monitoring data. In the previous studies, however, the real-time detection algorithm devised possesses only outlier identification and change detection abilities, without the function of damage extent assessment and uncertainty quantification.

The aim of this investigation is to develop a methodology for real-time defect detection of high-speed train wheels in the context of Bayesian DLM, which incorporates logics for prognosis, potential outlier detection, identification of change occurrence (change-point detection), and damage extent and uncertainty quantification. The Bayesian DLM is considered as a tool for time series analysis, while Bayesian forecasting is executed to enable the calculation of one-step ahead forecast distribution. The change-point detection is performed by checking the current observation against the routine model (forecast distribution generated by the Bayesian DLM for current instant) as well as against an alternative model of which the mean value is shifted by a prescribed offset. The detection rule is that if the alternative model better fits the actual observation, a potential change is signaled. To further determine whether such an observation is only an outlier or the beginning of an actual change (change-point), a specific logic is developed by introducing the Bayes factor and the maximum cumulative Bayes factor. Once the change-point is confirmed, Bayesian hypothesis testing is conducted for damage extent assessment and uncertainty quantification.

The main contributions of this study are the provision of: (i) a formula which not only enables the modeling of actual stress ranges derived from the monitoring data of strain but also forecasts the next observation distribution in the Bayesian framework; (ii) three metrics (i.e., the Bayes factor, maximum cumulative Bayes factor and run length) to allow for outlier and change-point detection in real-time manner; and (iii) an efficient way for damage extent assessment and uncertainty quantification. The rest of the article is organized as follows. Section 2 introduces the Bayesian DLM theory and an elaboration of the Bayesian forecasting philosophy. Section 3 presents the defect detection methodology that incorporates logics for outlier detection, change-point identification, and damage assessment. In Section 4, two case studies making use of time-

series strain data acquired by fiber Bragg grating (FBG) sensors affixed on the bogies of an in-service high-speed train are offered to demonstrate the feasibility and performance of the proposed methodology. Finally, conclusions are drawn in Section 5.

2. Bayesian DLM and forecasting

2.1. Bayesian DLM

The Bayesian DLM is a kind of process-based Bayesian prediction model which provides a flexible way to intuitively capture how processes evolve over time. It consists of two basic equations: an observation (measurement) equation and a system (evolution) equation [20,21]. The observation (measurement) equation describes the relationship between the observed data and the unknown state parameters. The system (evolution) equation represents the evolution of state parameters over time, thus illustrating the dynamic changes of the state variables. The two equations stated above are defined as [23]

$$\text{Observation Equation}: \quad y_t = F_t^{'}\theta_t + \nu_t, \qquad \nu_t \sim N[0, V_t] \tag{1a}$$

$$\text{System Equation}: \quad \theta_t = G_t\theta_{t-1} + \omega_t, \quad \omega_t \sim N[0, W_t] \tag{1b}$$

where y_t is the observation (measurement) vector ($m \times 1$) at time t; θ_t is unknown state parameter vector ($p \times 1$);F_t and G_t are the respective known regression matrix ($p \times m$) and evolution matrix ($p \times p$); ν_t and ω_t are two independent Gaussian random vectors with mean zero and unknown covariance matrices V_t and W_t. The DLM defined above amounts to treating θ_t as a Markov chain and y_t being independent conditionally on θ_t; that is, $\theta_t|\theta_{t-1}\tilde{N}(G_t\theta_{t-1}, W_t)$ and $y_t|\theta_t \sim N(F_t^{'}\theta_t, V_t)$.

The idea of describing a time series with DLM is to imagine the observation as obtained by combining simple elementary components, each capturing a series of diverse features, such as trend, seasonality (periodicity) and dependence on covariates (regression). The second order polynomial is a basic component for representing the trend of DLM, allowing for systematic growth or decline in level. The general expression of the second order polynomial DLM is [23]

$$y_t = \mu_t + \nu_t\,, \quad \nu_t \sim N(0, \sigma_{obs}^2) \tag{2a}$$

$$\mu_t = \mu_{t-1} + \alpha_{t-1} + \omega_{1t}\,, \quad \omega_{1t} \sim N(0, \sigma_{level}^2) \tag{2b}$$

$$\alpha_t = \alpha_{t-1} + \omega_{2t}\,, \quad \omega_{2t} \sim N(0, \sigma_{trend}^2) \tag{2c}$$

in which y_t is the real-time monitoring-derived stress range of a high-speed train bogie at time t, μ_t represents the stress range level at time t, and α_t represents the stress range change between time $t-1$ and t. ν_t is the zero-mean Gaussian random variable representing the error of measurement at moment t. ω_{1t} and ω_{2t} are both zero-mean Gaussian random variables representing the evolution of DLM from time $t-1$ to t. In association with the form of DLM in Equation (1), we have

$$\theta_t = \begin{pmatrix} \mu_t \\ \alpha_t \end{pmatrix}, \; F_t = \begin{pmatrix} 1 \\ 0 \end{pmatrix}, \; G_t = \begin{pmatrix} 1 & 1 \\ 0 & 1 \end{pmatrix}, \; W_t = \begin{pmatrix} \sigma_{level}^2 & 0 \\ 0 & \sigma_{trend}^2 \end{pmatrix}, \; V_t = \sigma_{obs}^2 \tag{3}$$

2.2. Bayesian forecasting

The Bayesian forecasting philosophy is based on the description of an observed process using its probability density function (PDF). As implied by the name, the Bayesian forecasting approach commences from Bayes' theorem, hence enabling the calculation of conditional probabilities. The details of using DLM for the recursive one-step ahead forecasting of the (posterior) distribution of monitoring-derived stress ranges under the Bayesian framework are presented as follows

Step 1 (initialization): Given the initial information D_0, the distribution of initial state parameters in the stress range is specified as

$$P(\theta_0|D_0) \sim N(m_0, C_0) \tag{4}$$

where m_0 and C_0 are initial mean and variance of the state parameters, which can be determined by using the first measured data of the time series in practice. Set $t = 0$.

Step 2 (a priori estimation): The posterior distribution of the state parameters at current time t, $P(\theta_t|D_t) \sim N(m_t, C_t)$, is employed to estimate the priori distribution of the state parameters at the next time $t+1$ as $P(\theta_{t+1}|D_t) \sim N(a_{t+1}, R_{t+1})$ with

$$a_{t+1} = E[\theta_{t+1}|D_t] = G_{t+1}m_t \tag{5a}$$

$$R_{t+1} = Var[\theta_{t+1}|D_t] = G_{t+1}C_tG_{t+1}^{'} + W_{t+1} \tag{5b}$$

where D_t denotes the state of information at time t; W_{t+1} is the variance of the evolution error in the system equation.

Step 3 (forecast): The mean and variance of the stress range distribution at next time $t+1$, $P(y_{t+1}|D_t) \sim N(f_{t+1}, Q_{t+1})$, can be forecasted through the observation equation,

$$f_{t+1} = E[y_{t+1}|D_t] = F'_{t+1} a_{t+1} \tag{6a}$$

$$Q_{t+1} = Var[y_{t+1}|D_t] = F'_{t+1} R_{t+1} F_{t+1} + V_{t+1} \tag{6b}$$

Step 4 (update): As time moves forward, once the new stress range y_{t+1} at time $t+1$ becomes available, the posterior distribution of the state parameters can be updated to $P(\theta_{t+1}|D_{t+1}) \sim N(m_{t+1}, C_{t+1})$, in which the mean and variance are given by

$$m_{t+1} = a_{t+1} + A_{t+1} e_{t+1} \tag{7a}$$

$$C_{t+1} = R_{t+1} - A_{t+1} A_{t+1}^T Q_{t+1} \tag{7b}$$

$$e_{t+1} = y_{t+1} - f_{t+1} \tag{7c}$$

$$A_{t+1} = R_{t+1} F_{t+1} / Q_{t+1} \tag{7d}$$

where $D_{t+1} = \{D_t, y_{t+1}\}$.

Step 5: Set $t = t+1$ and repeat the steps from Step 2 until to the end of the observation data. The recursive updating procedure is demonstrated in Fig. 1.

Note that in Step 4, A_{t+1} is the adaptive coefficient which can be viewed as the information tuner. It scales the correction term according to the relative variances of the prior and likelihood, as measured by R_{t+1}/Q_{t+1} and regressor value F_{t+1}. e_{t+1} is the one-step forward forecast error, the difference between the observed value y_{t+1} and its expectation f_{t+1}. More details about the recursive one-step ahead forecast method can be found in [24].

3. Defect detection methodology

The proposed defect detection methodology contains three logical processes: outlier detection, change-point detection, and damage assessment. By comparing the real-time measurement with the predicted values, the named outlier detection and change-point detection are devised to determine whether the measurement is a single outlier or the first observation of a remarkable change, the former being executed by calculating the Bayes factor, while the latter being based on the maximum cumulative Bayes factor. Once a change-point is affirmed, Bayesian hypothesis testing is conducted for further damage extent assessment and uncertainty quantification.

3.1. Outlier detection

Potential outlier detection is the first step in the process of the proposed defect detection approach, accomplished by the Bayes factor calculation. Bayes factor is advocated because of its straightforward and natural interpretation of evidence afforded by data. At every time step t, the Bayesian DLM can yield a PDF for the next measurement, labeled as M_0. Meanwhile, an artificial alternative model labeled as M_1 is defined by shifting the mean of M_0 by $+h$. The underlying idea of outlier detection is to check the current observation against both M_0 and M_1. For each time step t, the Bayes factor is the ratio of the PDF value under M_1 to the PDF value under M_0 [24],

$$H_t = \frac{p(y_t|D_{t-1}, M_1)}{p(y_t|D_{t-1}, M_0)} \tag{8}$$

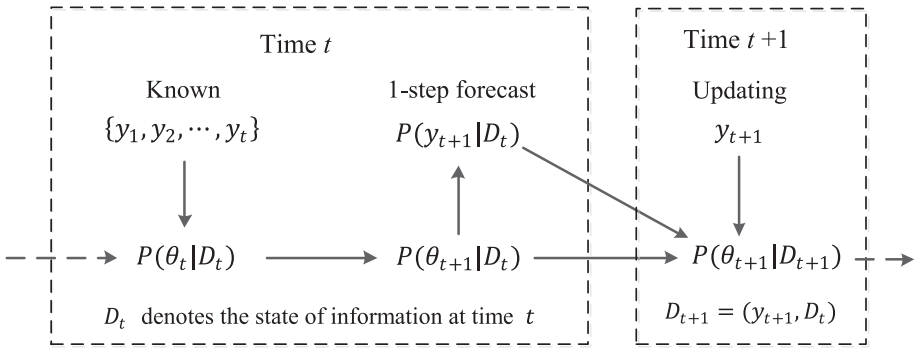

Fig. 1. Flowchart of DLM updating.

where y_t is the measurement at time t and D_{t-1} refers to the history information up to time $t-1$. In the case of Gaussian distributions, the Bayes factor is [25]

$$H_{1,t} = exp\left(\frac{2h(y_t - f_t) - h^2}{2\sigma_t^2}\right) \tag{9}$$

where h is the shift value; y_t is the observation value; f_t and σ_t are the mean and standard deviation of the forecasting distribution for observation at time t. A Bayes factor $H = 1$ indicates that the probability of the observation derived from model M_1 is identical to the probability of that derived from Model M_0. For better quantitative comparison between any two models, Jeffreys [36] suggested interpreting the Bayes factor as a scale of evidence and provided descriptive statements although the partitions are somewhat arbitrary. According to his suggestion, a Bayes factor can be divided into several intervals for assessing the significance of discrimination: $1 < H < 3$ is 'barely worth mentioning', $3 < H < 10$ is 'substantial', $10 < H < 30$ is 'strong', $30 < H < 100$ is 'very strong', and $H > 100$ is 'decisive'. In this study, $H_{min} = 10$ is set as a threshold for outlier detection.

In addition to the threshold of Bayes factor, the shift value h is also of concern, which can be determined by

$$h = \Phi^{-1}\left(\frac{1-\alpha}{2}\right) \times \sigma_t \tag{10}$$

where $\Phi^{-1}(\cdot)$ is the inverse of the standard normal cumulative distribution function, and α is the confidence level required. After the confirmation of H_{min} and h, an uncertainty limit (ucl) can be procured by the following equation

$$ucl = \frac{ln(H_{min})}{h}\sigma_t^2 + \frac{h}{2} \tag{11}$$

For instance, when the confidence level α and threshold of Bayes factor H_{min} are set as 90% and 10 respectively, the uncertainty limit $ucl = 2.22\sigma_t$. Thus, an observation is diagnosed as an outlier if its deviation from the mean value of M_0 is larger than $2.22\sigma_t$.

With the Bayes factor defined in Equation (9), only outliers with a positive deviation can be detected. To enable the outliers with negative deviation to be detected as well, a second Bayes factor is defined as

$$H_{2,t} = \exp\left(\frac{-2h(y_t - f_t) - h^2}{2\sigma_t^2}\right) \tag{12}$$

In the automatic monitoring process, both the Bayes factors $H_{1,t}$ and $H_{2,t}$ should be examined in parallel to enable the detection of both positive and negative outliers.

3.2. Change-point detection

In a dynamical system it is significant for an online diagnostic approach to maintain special vigilance on the most recent behavior, rather than judgments based on long past performances. Change-point is an abrupt variation in time series data, representing a transition that occurs between states. Change-point detection aims to detect abrupt change in the generative process of sequential data. It is assumed that a sequence of observations $y_1, \cdots, y_T$ could be divided into several non-overlapping partitions, e.g. dataset $j-1$, dataset j, and dataset $j+1$ as shown in Fig. 2. The delineations between partitions are known as change-points (e.g. TOC $j-1$ and TOC j); the goal of change-point detection is the determination of where the boundary of two adjacent partitions is located in a sequence of observations. Change-point detection approaches can be classified into offline and online methods. The former needs to observe the whole sequential observations before aiming to make inference on the generative process of the sequence [37–40], wheras the latter aims to update the inference at each time step with the newly acquired measurements from the sequence [41–43]. In particular, the Bayesian online change-point detection methods are based on computing the probability distribution of the run length.

The outlier detection method stated in the previous sub-section is confined to single-point outlier recognition and cannot differentiate between the single-point outlier and the beginning of a continual change. To overcome this problem, cumulative Bayes factor (local Bayes factors) is recommended to detect change-point(s) in the sequence of observations, by defining it as the product of k consecutive Bayes factors

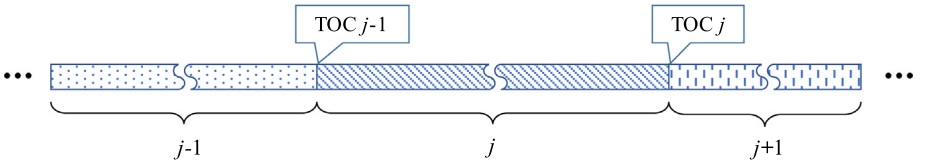

Fig. 2. Sequence of observations obtained under different conditions.

$$H_t(k) = \prod_{t-k+1}^{t} H_t\,, \quad k = 1, 2, \cdots, l_{max} \tag{13}$$

where l_{max} is the maximum number of Bayes factors taken into account. Unlike Bayes factor with implicitly no historical influence in the judgement, the consecutive Bayes factors collect evidence of change over a series of observation (from time $(t-k+1)$ to time t). That is, $H_t(k)$ measures the evidence provided by the most recent k consecutive observations. The maximal cumulative Bayes factor is defined as

$$L_t = \max\left(H_t(k)\right) = H_t(l_t) \tag{14}$$

where l_t refers to the run length which counts the number of recent, consecutive observations that contribute to the maximum value of L_t. It can be calculated recursively by

$$l_t = \begin{cases} 1, & if\ L_{t-1} \le 1 \\ 1 + l_{t-1}, & if\ L_{t-1} > 1 \end{cases} \tag{15}$$

initialized with $L_0 = 1$ and $l_0 = 1$. The sequence of L_t provides the basis of a local monitoring scheme, with the run length l_t indicating how long ago the change might have begun. The rational run length threshold of l_t is suggested as $l_{min} = 4$ by Pole et al. [23]. Akin to the Bayes factor threshold for outlier detection, the threshold of maximal cumulative Bayes factors is set as $L_{min} = 10$. If the conditions $L_t > L_{min}$ and $l_t > l_{min}$ occur simultaneously, an alarm of change is immediately issued at time t (time of notification, *TON*). The real time of occurrence (*TOC*) is $(t - l_t + 1)$, that is, $TOC = t - l_t + 1$.

3.3. Damage extent assessment

Once the change-point is confirmed, Bayesian hypothesis testing is performed to assess damage extent and quantify the associated uncertainty. The proposed approach directly quantifies the likelihoods of two scenarios (e.g., the sequential observations before and after the change-point), that is, "no fault" and "fault", and the yielded results are easy to interpret. An additional merit of the proposed approach is its ability to quantify the uncertainty in damage detection. Assume that the observed sequential data can be divided into two non-overlapping partitions, the first of which is regarded as healthy and conforms to a normal distribution $N(\mu_0, \sigma_0^2)$, while the second is deemed as damage complying with a normal distribution $N(\mu_1, \sigma_1^2)$. In this study, the variance σ_1^2 is assumed as equal to σ_0^2, and the hypothesis testing is made only on the mean of the observations. Thus, the damage detection problem becomes the test of $H_0 : \mu = \mu_0$ versus $H_1 : \mu \neq \mu_0$ with $\mu|H_1 \sim N(\rho, \tau^2)$, where ρ and τ^2 are two parameters of the prior density of μ under the alternative hypothesis. The null hypothesis H_0 indicates that the structure is healthy, while the alternative hypothesis H_1 indicates that the structure is damaged.

With the above, damage detection can be achieved by means of Bayes factor which is defined as the ratio of the probability of observations given the alternate hypothesis to the probability of observations given the null hypothesis [24]

$$BF(H_1 : H_0) = B_{10} = \frac{P(D|H_1)}{P(D|H_0)} \tag{16}$$

where $D = \{y_1, \cdots, y_n\}$ refers to the observed data. It is proven to be [44]

$$BF(H_1 : H_0) = B_{10} = \left(\frac{\tau^2 + \sigma_0^2/n}{\sigma_0^2/n}\right)^{-1/2} \exp\left\{\frac{n}{2}\left[-\frac{(\overline{y} - \rho)^2}{\sigma_0^2 + n\tau^2} + \frac{(\overline{y} - \mu_0)^2}{\sigma_0^2}\right]\right\} \tag{17}$$

where $\overline{y}$ refers to the mean of the observed data $\{y_1, \cdots, y_n\}$. If no prior information is available, the initial mean and variance can be set as $\rho = \mu_0$ and $\tau^2 = \sigma_0^2$ [44]. The two assumptions take the prior mean and variance in the alternative hypothesis as equal to the values of null hypothesis. Then the Bayes factor is

$$B_{10} = (n+1)^{-1/2} \exp\left\{\frac{n}{n+1}\frac{z^2}{2}\right\} \tag{18}$$

where $z = \sqrt{n}\frac{\overline{y} - \mu_0}{\sigma_0}$. At each time step (i.e., n=1), the Bayes factor B_{10} is larger for the larger values of $|z|$, which is reasonable and easy to interpret. The logarithm of the Bayes factor, for convenience of comparison among a larger of values, is derived as

$$\log B_{10} = -\frac{1}{2}\log(n+1) + \frac{nz^2}{2(n+1)} \tag{19}$$

If the Bayes factor B_{10} is larger than 1, the implication is that the observed data provide evidence in favor of the alternative hypothesis H_1 (i.e., the structure is damaged). Otherwise, the observed data are judged to support the null hypothesis H_0 (i.e., the structure is healthy). As with the previous threshold, $B_{10} \ge 10$ is set as a threshold for damage indication.

With the proposed approach, the uncertainty in damage detection can be quantitatively assessed by the posterior probability of the alternative hypothesis $p(H_1|D)$. It can be derived as

$$p(H_1|D) = \frac{p(D|H_1)p(H_1)}{p(D|H_0)p(H_0) + p(D|H_1)p(H_1)} = \frac{B_{10}p(H_1)}{p(H_0) + B_{10}p(H_1)} \tag{20}$$

where $p(H_1)$ and $p(H_0)$ denote the prior probabilities of the hypotheses H_1 and H_0, respectively. Due to the absence of any prior information concerning the two hypotheses, it usually lets $p(H_1) = p(H_0) = 0.5$. In such circumstance, Eq. (20) reduces to

$$p(H_1|D) = \frac{B_{10}}{1 + B_{10}} \tag{21}$$

$B_{10} \to 0$ indicates 0% confidence in accepting the alternative hypothesis, and $B_{10} \to \infty$ indicates 100% confidence. The above equation gives a direct metric of the probability of damage and it is also easy to compute and interpret.

Integrating together the outlier detection, change-point detection and damage assessment, the implementation procedures of the proposed methodology are shown in Fig. 3. Beginning at time t, the single Bayes factor is firstly evaluated to judge whether y_t is an outlier. If not, the maximum cumulative Bayes factor L_t and run length l_t for change-point detection are calculated. Once a change-point is detected, the intervention is carried out by resetting the time to the time of occurrence (i.e., $TOC = t - l_t + 1$) and by adjusting the mean value of M_0 to the observation y_t (i.e., $f_t = y_t$), and the subsequent analysis will then be started at *TOC*. Meanwhile, Bayesian hypothesis testing is executed for damage extent assessment and uncertainty quantification from the current *TOC* to the next *TOC*.

4. Application to in-service monitoring data of high-speed train

4.1. Onboard monitoring system

An onboard monitoring system has been designed and implemented on an in-service high-speed passenger train running on the Lanzhou-Urumqi High-Speed Railway (LUHSR) in China [45]. As shown in Fig. 4, the monitoring system is composed of a total of 52 FBG strain sensors, 4 FBG temperature sensors, 11 accelerometers (tri-axial) and 1 noise sensor deployed on both motor and trailer bogies. Also, one tri-axial FBG accelerometer, one video camera and two GPS sensors are installed inside a train carriage. As the present work is focused on the real-time detection of potentially defective wheels by using strain monitoring data from bogies, only the deployment of strain sensors is concerned. The strain sensors are mounted on 4 measurement zones of the bogies: (i) the zone with the action of high loads; (ii) the stress transmission zone; (iii) the zone with high responses predicted by finite element analysis; and (iv) welded joints. FBG strain (and temperature) sensors are deployed and attached to the surface of the train bogie with industrial glue and tapes, and connected to the interrogator (data logger) with laptop inside the train carriage through optical fiber cables.

The data utilized in this study were obtained from a monitoring schedule spanning 18 days as shown in Table 1. The total length of the LUHSR between Lanzhou and Urumqi is 1777 km. In the trip from Lanzhou to Urumqi, the high-speed train stops by 14 stations and travels cross 13 railroad sections (e.g. 1st, 2nd, ..., 13th); in trip from Urumqi to Lanzhou, the high-speed train stops by 15 stations and travels cross 14 railroad sections (e.g. 1st, 2nd, ..., 14th). During the monitoring period, the train operated at its normal speed around 200–250 km/h. The sampling rate for all the sensors was set at 5000 Hz.

Since the train wheels were lathed (lathing is a process to make wheels perfectly rounded) during the monitoring period, the recorded data contain information in line with two different states (before lathing and after lathing). The wheels can be considered as potentially unhealthy (defective) before lathing and as healthy after lathing. To verify the effectiveness of the

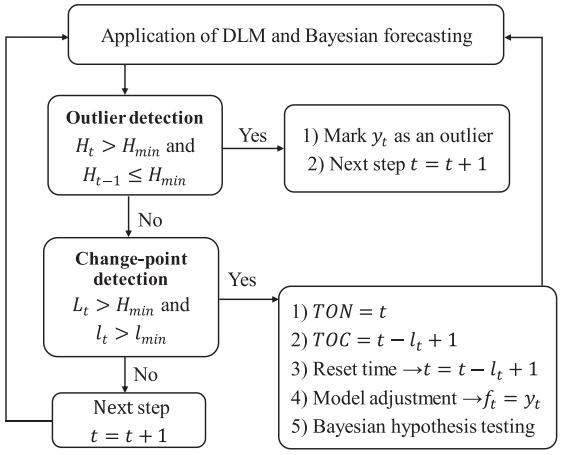

Fig. 3. Flowchart of defect detection framework.

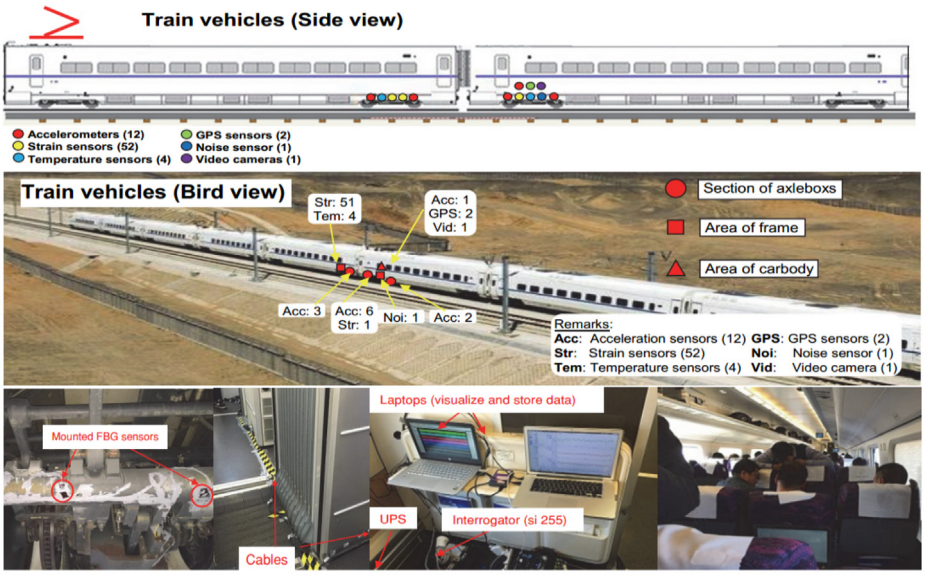

(a) Layout of deployed sensors

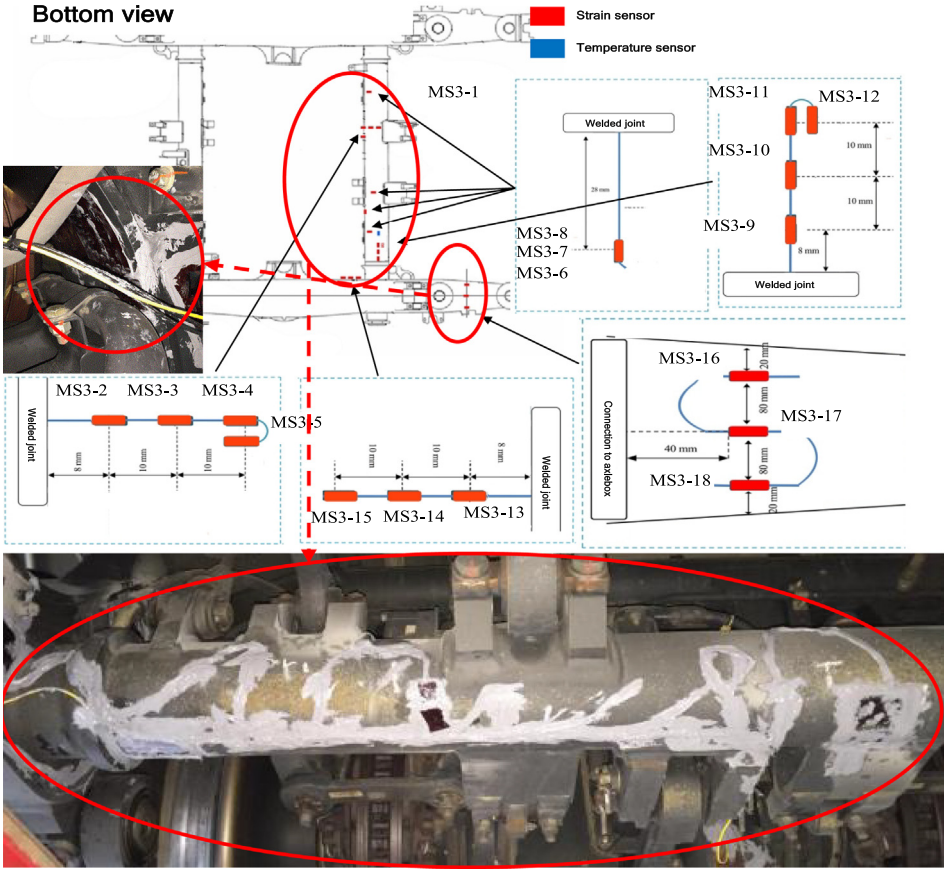

(b) Locations of FBG strain sensors deployed on a bogie

Fig. 4. In-service monitoring of a high-speed passenger train.

proposed real-time defect detection methodology, the strain monitoring data obtained from the bogies before and after wheel lathing are used in the study.

Table 1
Monitoring schedule for instrumented high-speed train.

Train Conditions	Time	Type of Work
Before wheel lathing	20 ~ 21 Dec 2015	Installation (2 days)
	22 ~ 31 Dec 2015	Onboard monitoring (10 days)
	1 ~ 2 Jan 2016	Wheel lathing (2 days)
After wheel lathing	3 ~ 10 Jan 2016	Onboard monitoring (8 days)
	11 ~ 13 Jan 2016	Regular maintenance (2 days)
	14 Jan 2016	Urban route (1 day)

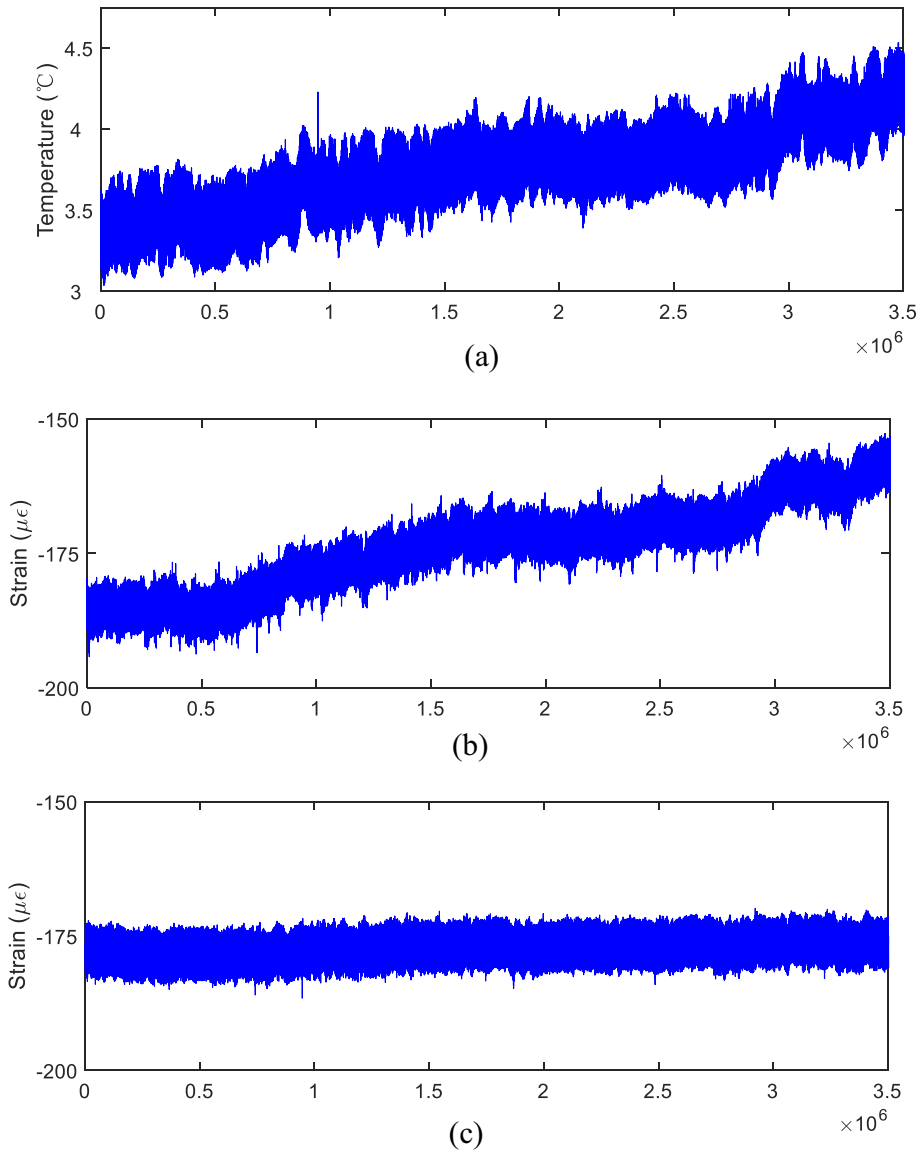

Fig. 5. Time histories of temperature, strain before and after temperature compensation: (a) measured temperature; (b) measured strain response; (c) strain response after temperature compensation.

4.2. Data processing

The train's dynamic responses may be influenced by different subgrade conditions of the railroad, such as ground, tunnel, and bridge. To eliminate the effects of different railroad conditions, the strain data recorded from the same railroad section

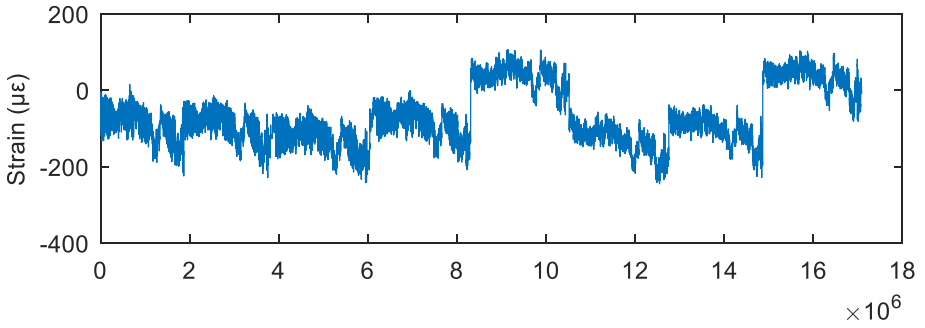

Fig. 6. Measured strain responses (Case 1).

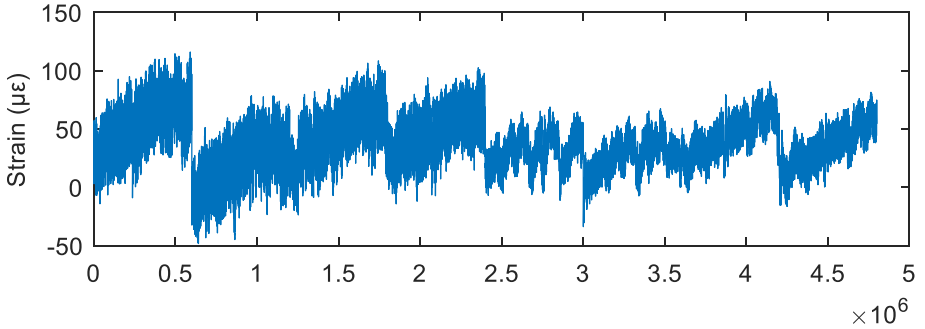

Fig. 7. Measured strain responses (Case 2).

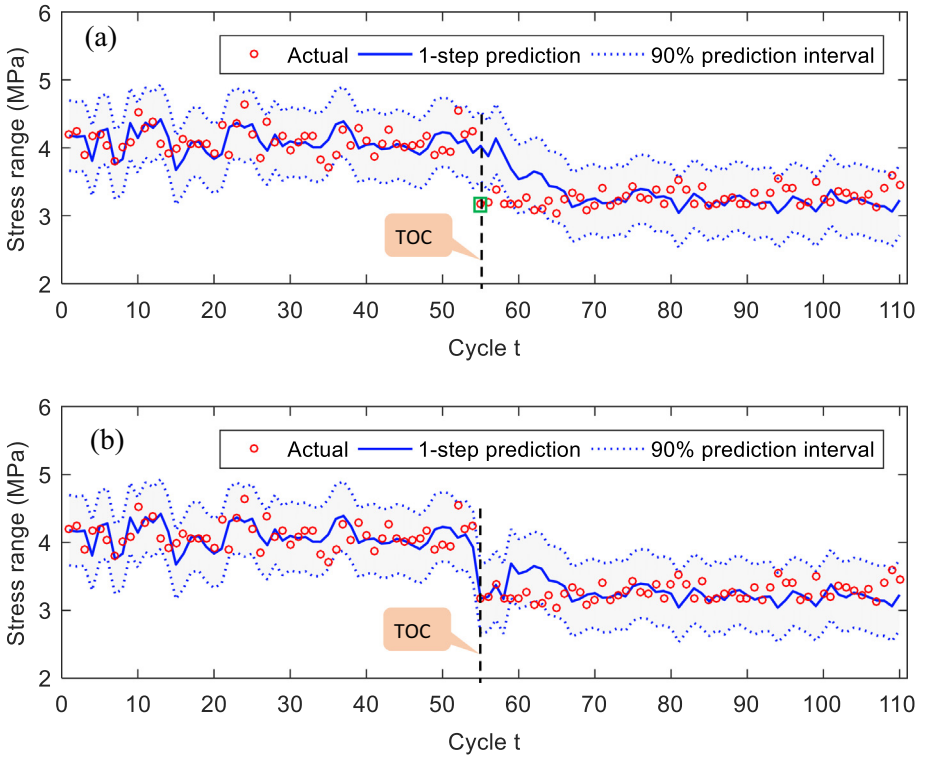

Fig. 8. Bayesian DLM-based forecasts of stress range for Case 1: (a) before adjustment; (b) after adjustment.

before and after lathing, are used in each scenario. In addition, the passenger loads in different trips are deemed statistically identical and the speed of train is assumed to be constant as in normal operation. Without loss of generality, the monitoring data respectively obtained from two typical railroad sections (1st and 14th) in the trip from Urumqi to Lanzhou are chosen to illustrate the proposed real-time defect detection methodology, which are from the strain gauge (MS3-7) deployed at the tubular crosspiece (Fig. 4b).

For the sake of brevity, the monitoring data collected from the 1st railroad section are denoted as Case 1, while those from the 14th railroad section are denoted as Case 2. Firstly, the measured strain is converted to stress for the subsequent stress range calculation. For the strain gauges mounted on the steel surface, the conversion of the measured strain to stress is made by $\sigma_s = E\varepsilon$, where E is the elasticity modulus of steel and ε is the strain after eliminating the effect of varying temperatures. The equation of temperature compensation is defined as

$$\varepsilon = \varepsilon_m - a_1(T_m - T_0) \tag{22}$$

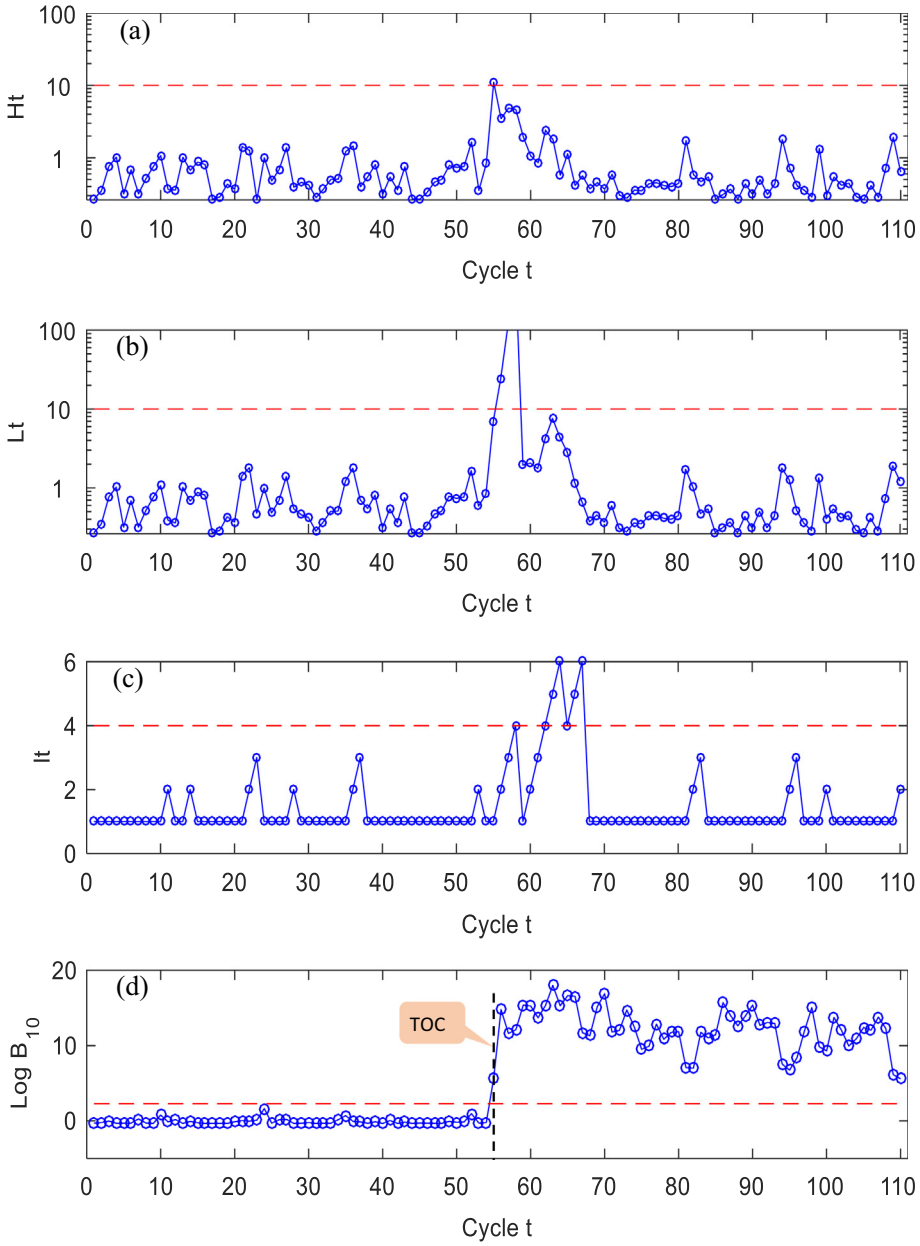

Fig. 9. Detection results for Case 1: (a) Bayes factor; (b) maximal cumulative Bayes factor; (c) run length; (d) Bayesian hypothesis testing.

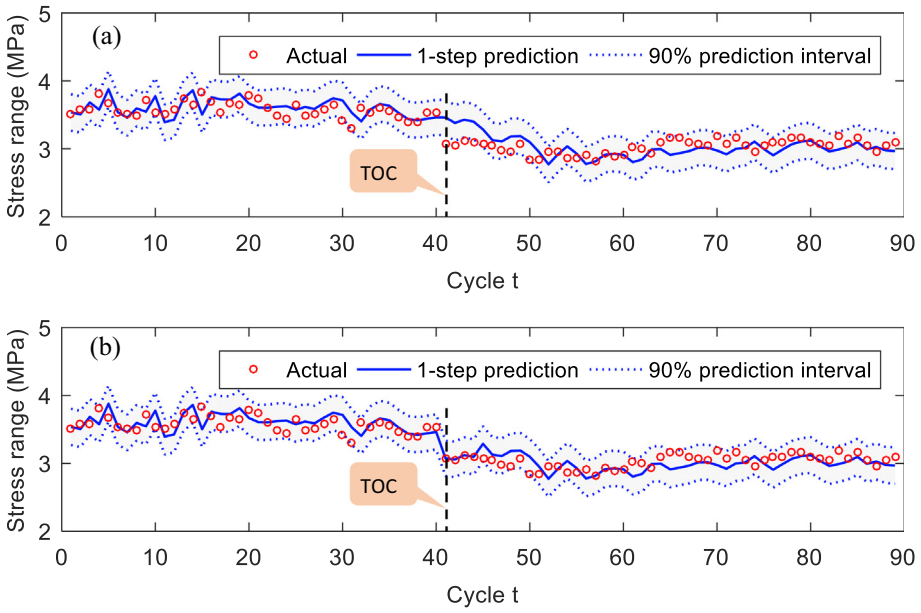

Fig. 10. Bayesian DLM-based forecasts of stress range for Case 2: (a) before adjustment; (b) after adjustment.

where ε_m is the measured strain, T_m is the measured temperature in the vicinity of the strain sensor, T_0 is the temperature at the installation, and a_1 is a constant coefficient. In our case, the original temperature is 4 , i.e., $T_0 = 4$. The results of temperature compensation are demonstrated in Fig. 5. It is obvious that the trend in strain responses caused by temperature change has been eliminated.

Afterwards, the stress ranges are extracted from the monitoring-derived stress data by the application of the rainflow counting algorithm. From each stress cycle, the stress range S_a is obtained by calculating the difference between the maximum stress σ_{max} and the minimum stress σ_{min} measured in that stress cycle, i.e., $S_a = \sigma_{max} - \sigma_{min}$. More details on the stress ranges extraction are given in [45]. The stress ranges with amplitudes lower than 1 MPa need to be culled because the majority are caused by noise. To decrease the uncertainty arising from the measurement facilities, the average stress ranges for every ten minutes are used as the target quantities. Due to the different lengths of the two selected railroad sections (1st and 14th), the traveling time of the train in each section is also different. This results in different data lengths. The data lengths of the average stress ranges in Case 1 and Case 2 are 110 and 90, respectively. Figs. 6 and 7 show the original measured strain responses before and after lathing in Case 1 and Case 2, respectively.

4.3. Analysis results and discussion

Following the implementation procedures mentioned before, the defect detection results for Case 1 are demonstrated in Figs. 8 and 9. Fig. 8(a) shows the average stress range (red point) together with 1-step ahead prediction (blue solid line) and the corresponding 90% prediction interval (grey shadow). It is observed that, although some observations at the time interval $t \in [55, 59]$ fall outside the 90% prediction interval, only the Bayes factor at time $t = 55$ exceeds the established threshold of $H_{min} = 10$ as shown in Fig. 9(a). It is thus judged as an outlier (marked as □). The reason is that because when applying the proposed approach, the shift parameter is set as $h = 1.645\sigma_t$, resulting in the uncertainty limit $ucl = 2.22\sigma_t$ while the other four observations are still within the uncertainty limit. On the other hand, Fig. 9(b)–(c) shows the results of the maximum cumulative Bayes factor and the corresponding run length for change detection. It is seen that the maximum cumulative Bayes factor values at time instants $t = 56,\ 57$ and 58 are larger than the threshold of $L_{min} = 10$, while merely the run length at instant $t = 58$ surpasses the threshold of $l_{min} = 4$. Apparently, this observation at time $t = 58$ fulfills the conditions of change-point detection causing an alarm to be issued (i.e., $TON = 58$). The identified real occurrence time of change-point is $t = 55$ (i.e., $TOC = 58 - 4 + 1 = 55$), which coincides well with the actual time point of lathing the wheels. In accordance with the real-time identification of change-point occurrence, the prediction model is refined by altering the guessed mean value at *TOC*, as shown in Fig. 8(b). The predictions near *TOC* in the refined model obviously agree well with the actual observations, thus offering a better prediction performance than that of the original model.

The results of defect detection by means of Bayesian hypothesis testing are illustrated in Fig. 9(d). The discrimination between "healthy" and "defective" is quantified by the logarithm value of Bayes factor. It is seen from Fig. 9(d) that the vast majority of logarithm values of Bayes factor before *TOC* are nearly zero and below the threshold level (dotted red line), which advocate the hypothesis of "healthy state" (no defect). This is consistent with the actual health condition and thus validates

the capability of the Bayesian hypothesis testing. On the contrary, all the logarithm values of Bayes factor after *TOC* are larger than 2, meaning that the corresponding Bayes factor values exceed 100. According to the classification of Bayes factor stipulated in Sub-section 3.1, this result ($H > 100$) favors the hypothesis of "damage existence" and the damage severity is classified as "decisive". Indeed, wheels immediately before being sent to depot for lathing were in the state of 'heavily defective'. Making use of Eq. (21), the probabilities of damage after *TOC* are obtained as 100%, that is, the wheels are identified as defective with a very high confidence.

The defect detection results for Case 2 are similar to Case 1, and are illustrated in Figs. 10 and 11. As seen in Fig. 11(a)–(c) no outlier exists throughout the whole period, but a change-point is identified, of which the time of notification is $t = 44$ (i.e., $TON = 44$) and the real time of occurrence is $t = 41$ (i.e., $TOC = 44 - 4 + 1 = 41$). The result matches well with the actual time point when wheel lathing is inflicted. For the predictions near the change-point, the modified prediction model (Fig. 10(b)) offers a better performance than the original model (Fig. 10(a)). As illustrated in Fig. 11(d), all the logarithm values of Bayes factor after *TOC* are larger than the threshold (dotted red line), whereas the values before *TOC* are within the

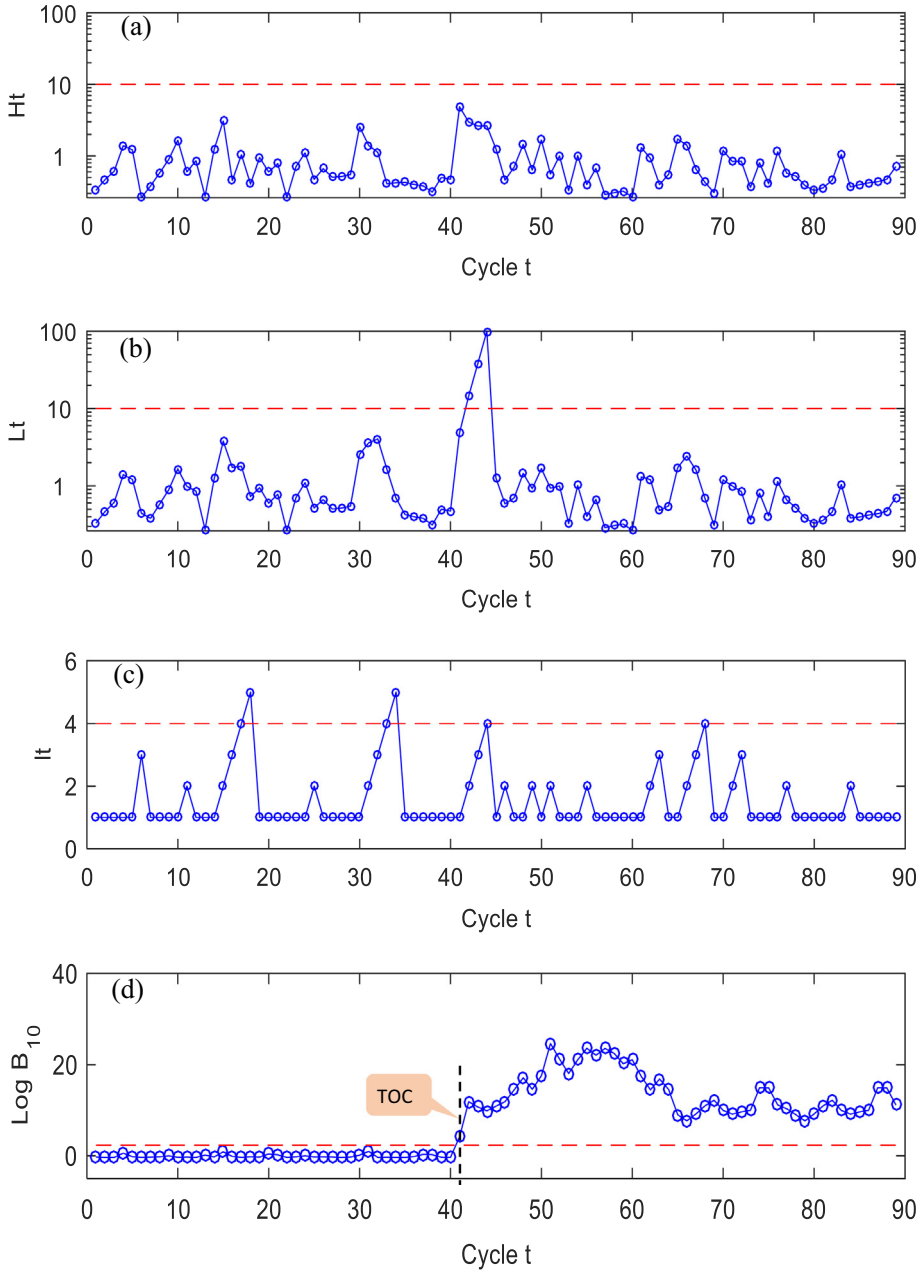

Fig. 11. Detection results for Case 2: (a) Bayes factor; (b) maximal cumulative Bayes factor; (c) run length; (d) Bayesian hypothesis testing.

threshold line. The values of Bayes factor after *TOC* are obtained to be higher than 100 ($H > 100$) and the corresponding probabilities of damage are approximately 100%, which advocate the hypothesis of "damage existence" and the damage severity is classified as "decisive".

Apart from the accuracy of the proposed approach, the computational efficiency is also of concern. The algorithmic implementation is performed on a Lenovo ThinkCentre M720t desktop (Lenovo, Beijing, China) with Dual Intel Core i7-8700 processor (Intel, California, USA) and 24 GB of memory. The computation times consumed in Case 1 and Case 2 are 4.0109 s and 3.7704 s respectively. In this sense, it realizes the detection of wheel defects in real time.

5. Conclusions

A novel methodology for real-time defect detection of high-speed train wheels using Bayesian forecasting and dynamic linear model (DLM) has been developed and validated in this study. First, the DLM is formulated to approximate the actual stress range derived from the strain monitoring data and to obtain forecast distribution for next observation in the Bayesian framework. Afterwards, three metrics (i.e., Bayes factor, maximum cumulative Bayes factor and run length) are elicited for outlier detection and change-point detection. After the change-point has been confirmed, damage assessment is executed by the Bayesian hypothesis testing of the sequential observations before and after the change-point. Due to accommodating the dynamic evolution process and the statistical nature of the method, the proposed approach not only possesses the ability of real-time damage detection, but also enables damage quantification (through classifying the range of Bayes factor) and uncertainty assessment (through calculating the probability of damage). The methodology is illustrated by using the online monitoring data of strain from high-speed train bogies acquired under different wheel conditions (before and after wheel lathing). In the two cases addressed, wheel defects are successfully identified, hence validating the effectiveness of the developed method. The quantitative results about the damage extent and confidence would provide useful information helping to make cost-effective, risk-based decisions with the aim of maintaining the operation safety of high-speed rail.

Despite the proposed methodology being developed for wheel defect detection of high-speed trains, it can also be applied to low-speed passenger and freight trains as well as extended to SHM for a wide variety of civil infrastructure (e.g., bridges, buildings and tunnels) when vibration signals are available via monitoring. In this study, the second-order polynomial DLM is employed to model the stress ranges, which only considers the change of stress range level and trend. However, most long-term SHM data, especially long-term strain monitoring data, are generally contaminated by trend, seasonal (cyclical) and regression effects, which require a more complex model. The Bayesian DLM enables the modeling of time-dependent responses of a structure by integrating appropriate components, for instance, the response with cyclical characteristics can be depicted by embedding a seasonal (cyclical) component. Thus, in accordance with the nature of monitoring data, an appropriate Bayesian DLM enabling to describe time series data of different features, can be formulated for damage detection of a variety of structures subject to different operational/environmental conditions.

CRediT authorship contribution statement

Y.W. Wang: Methodology, Software, Formal analysis, Investigation, Writing - original draft, Visualization. **Y.Q. Ni:** Conceptualization, Resources, Writing - review & editing, Supervision, Project administration, Funding acquisition. **X. Wang:** Data curation, Validation.

Declaration of Competing Interest

The authors declare that they have no known competing financial interests or personal relationships that could have appeared to influence the work reported in this paper.

Acknowledgements

The work described in this paper was supported by a grant from the Research Grants Council of the Hong Kong Special Administrative Region, China (Project No. PolyU 152024/17E). The authors would also like to appreciate the funding support by the Innovation and Technology Commission of Hong Kong SAR Government to the Hong Kong Branch of Chinese National Rail Transit Electrification and Automation Engineering Technology Research Center (Grant No. K-BBY1).

References

[1] S. Dietz, H. Netter, D. Sachau, Fatigue life prediction of a railway bogie under dynamic loads through simulation, Veh. Syst. Dyn. 29 (1998) 385–402, https://doi.org/10.1080/00423119808969381.
[2] S. Iwnicki, Handbook of Railway Vehicle Dynamics, CRC Press, Florida, USA, 2006, doi:10.1201/9781420004892.
[3] A. Johansson, J.C.O. Nielsen, Out-of-round railway wheels wheel-rail contact forces and track response derived from field tests and numerical simulations, J. Rail Rapid Transit 217 (2003) 135–146.
[4] D. Barke, W.K. Chiu, Structural health monitoring in the railway industry: a review, Struct. Health Monit. 4 (2005) 81–93, https://doi.org/10.1177/1475921705049764.

[5] S.Y. Chong, J.R. Lee, H.J. Shin, A review of health and operation monitoring technologies for trains, Smart Struct. Syst. 6 (2010) 1079–1105, https://doi.org/10.12989/sss.2010.6.9.1079.
[6] J. Pombo, J. Ambrosio, M. Pereira, R. Lewis, Development of a wear prediction tool for steel railway wheels using three alternative wear functions, Wear 271 (2011) 238–245, https://doi.org/10.1016/j.wear.2010.10.072.
[7] J. Pombo, J. Ambrósio, M. Pereira, R. Lewis, R. Dwyer-Joyce, C. Ariaudo, N. Kuka, A study on wear evaluation of railway wheels based on multibody dynamics and wear computation, Multibody Sys. Dyn. 24 (2010) 347–366, https://doi.org/10.1007/s11044-010-9217-8.
[8] A.R. Andrade, J. Stow, Statistical modelling of wear and damage trajectories of railway wheelsets, Qual. Reliab. Eng. Int. 32 (2016) 2909–2923, https://doi.org/10.1002/qre.1977.
[9] A. Alemi, F. Corman, G. Lodewijks, Condition monitoring approaches for the detection of railway wheel defects, J. Rail Rapid Transit 231 (2017) 961–981, https://doi.org/10.1177/0954409716656218.
[10] B.W. Drinkwater, P.D. Wilcox, Ultrasonic arrays for non-destructive evaluation: a review, NDT E Int. 39 (2006) 525–541, https://doi.org/10.1016/j.ndteint.2006.03.006.
[11] A.G. Verkhoglyad, I.N. Kuropyatnik, V.M. Bazovkin, G.L. Kuryshev, Infrared diagnostics of cracks in railway carriage wheels, Russ. J. Nondestr. Test. 44 (2008) 664–668, https://doi.org/10.1134/S1061830908100021.
[12] Z.H. Żurek, K. Bizon, B. Rockstroh, Supplementary magnetic tests for railway wheel sets, Transport Problems 3 (2008) 5–10.
[13] A. Matsumoto, Y. Sato, H. Ohno, M. Tomeoka, K. Matsumoto, J. Kurihara, T. Ogino, M. Tanimoto, Y. Kishimoto, Y. Sato, T. Nakai, A new measuring method of wheel–rail contact forces and related considerations, Wear 265 (2008) 1518–1525, https://doi.org/10.1016/j.wear.2008.02.031.
[14] R.S. Dwyer-Joyce, C. Yao, R. Lewis, H. Brunskill, An ultrasonic sensor for monitoring wheel flange/rail gauge corner contact, J. Rail Rapid Transit 227 (2013) 188–195, https://doi.org/10.1177/0954409712460986.
[15] B. Frankenstein, D. Hentschel, E. Pridoehl, F. Schubert, Hollow shaft integrated health monitoring system for railroad wheels, Proceeding of Advanced Sensor Technologies for Nondestructive Evaluation and Structural Health Monitoring, 2005.
[16] B. Liang, S.D. Iwnicki, Y. Zhao, D. Crosbee, Railway wheel-flat and rail surface defect modelling and analysis by time–frequency techniques, Veh. Syst. Dyn. 51 (2013) 1403–1421, https://doi.org/10.1080/00423114.2013.804192.
[17] B. Stratman, Y. Liu, S. Mahadevan, Structural health monitoring of railroad wheels using wheel impact load detectors, J. Fail. Anal. Prev. 7 (2007) 218–225, https://doi.org/10.1007/s11668-007-9043-3.
[18] C.C. Lai, J.C.P. Kam, D.C.C. Leung, T.K.Y. Lee, A.Y.M. Tam, S.L. Ho, H.Y. Tam, M.S.Y. Liu, Development of a fiber-optic sensing system for train vibration and train weight measurements in Hong Kong, J. Sensors 2012 (2012) 365165.
[19] H.J. Salzburger, M. Schuppmann, L. Wang, X. Gao, In-motion ultrasonic testing of the tread of high-speed railway wheels using the inspection system AUROPA III, Insight-Non-Destruct. Testing Condition Monit. 51 (2009) 370–372, https://doi.org/10.1784/insi.2009.51.7.370.
[20] M.L. Lee, W.K. Chiu, Determination of railway vertical wheel impact magnitudes: field trials, Struct. Health Monit. 6 (2007) 49–65, https://doi.org/10.1177/1475921707072063.
[21] K. Bollas, D. Papasalouros, D. Kourousis, A. Anastasopoulos, Acoustic emission monitoring of wheel sets on moving trains, Constr. Build. Mater. 48 (2013) 1266–1272, https://doi.org/10.1016/j.conbuildmat.2013.02.013.
[22] K. Yang, L. Ma, X. Gao, L. Wang, Profile parameters of wheelset detection for high speed freight train, Proceedings of Fourth International Conference on Digital Image Processing (ICDIP 2012), 2012.
[23] A. Pole, M. West, J. Harrison, Applied Bayesian Forecasting and Time Series Analysis, CRC Press, New York, USA, 1994.
[24] M. West, J. Harrison, Bayesian Forecasting and Dynamic Models, Springer-Verlag, New York, USA, 1997, doi:10.1007/b98971.
[25] H. Lipowsky, S. Staudacher, M. Bauer, K.J. Schmidt, Application of Bayesian forecasting to change detection and prognosis of gas turbine performance, J. Eng. Gas Turbines Power 132 (2010), https://doi.org/10.1115/1.3159367 031602.
[26] X. Fei, C.C. Lu, K. Liu, A Bayesian dynamic linear model approach for real-time short-term freeway travel time prediction, Transport. Res. Part C: Emerging Technol. 19 (2011) 1306–1318, https://doi.org/10.1016/J.TRC.2010.10.005.
[27] J. Gill, Bayesian Methods: A Social and Behavioral Sciences Approach, third ed., Chapman and Hall/CRC, New York, USA, 2014, doi:10.1201/b17888.
[28] M. Laine, N. Latva-Pukkila, E. Kyrölä, Analysing time-varying trends in stratospheric ozone time series using the state space approach, Atmos. Chem. Phys. 14 (2014) 9707–9725, https://doi.org/10.5194/acp-14-9707-2014.
[29] X. Fan, Y. Liu, Combinatorial Bayesian dynamic linear models of bridge monitored data and reliability prediction, Chin. J. Eng. 2016 (2016), https://doi.org/10.1155/2016/3648126.
[30] F. Sun, N. Wang, X. Li, W. Zhang, Remaining useful life prediction for a machine with multiple dependent features based on Bayesian dynamic linear model and copulas, IEEE Access 5 (2017) 16277–16287, https://doi.org/10.1109/ACCESS.2017.2735966.
[31] G. Petris, S. Petrone, P. Campagnoli, Dynamic Linear Models with R, Springer, New York, USA, 2009, doi:10.1007/b135794_1.
[32] J.A. Goulet, Bayesian dynamic linear models for structural health monitoring, Struct. Control Health Monit. 24 (2017), https://doi.org/10.1002/stc.2035 e2035.
[33] J.A. Goulet, K. Koo, Empirical validation of Bayesian dynamic linear models in the context of structural health monitoring, J. Bridge Eng. 23 (2018) 05017017, https://doi.org/10.1061/(ASCE)BE.1943-5592.0001190.
[34] Y.W. Wang, Y.Q. Ni, X. Wang, Detection of performance of high-speed train wheels based on Bayesian dynamic model, Proceedings of the 11th International Workshop on Structural Health Monitoring, DEStech Publications, 2017.
[35] L.H. Zhang, Y.W. Wang, Y.Q. Ni, S.K. Lai, Online condition assessment of high-speed trains based on Bayesian forecasting approach and time series analysis, Smart Struct. Syst. 21 (2018) 705–713.
[36] H. Jeffreys, Theory of Probability, third ed., Oxford Clarendon Press, Oxford, UK, 1961.
[37] D. Barry, J.A. Hartigan, A Bayesian analysis for change point problems, J. Am. Stat. Assoc. 88 (1993) 309–319, https://doi.org/10.2307/2290726.
[38] S. Chib, Estimation and comparison of multiple change-point models, J. Econ. 86 (1998) 221–241, https://doi.org/10.1016/S0304-4076(97)00115-2.
[39] R. Killick, P. Fearnhead, I.A. Eckley, Optimal detection of changepoints with a linear computational cost, J. Am. Stat. Assoc. 107 (2012) 1590–1598, https://doi.org/10.1080/01621459.2012.737745.
[40] R. Maidstone, T. Hocking, G. Rigaill, P. Fearnhead, On optimal multiple changepoint algorithms for large data, Stat. Comput. 27 (2017) 519–533, https://doi.org/10.1007/s11222-016-9636-3.
[41] P. Fearnhead, Exact and efficient Bayesian inference for multiple changepoint problems, Stat. Comput. 16 (2006) 203–213, https://doi.org/10.1007/s11222-006-8450-8.
[42] R.P. Adams, D.J.C. MacKay, Bayesian online changepoint detection, (2007). https://arxiv.org/abs/0710.3742.
[43] M. Byrd, L. Nghiem, J. Cao, Lagged exact Bayesian online changepoint detection, (2017). http://arxiv.org/abs/1710.03276.
[44] H.S. Migon, D. Gamerman, Statistical Inference: An Integrated Approach, Oxford University Press, New York, USA, 1999, doi:10.1002/sim.898.
[45] X. Wang, Y.Q. Ni, Analysis of influence of mean stress on fatigue life of in-service high-speed train bogies using monitoring data, Proceedings of the 3rd International Conference on Railway Technology: Research, Development and Maintenance, 2016.